Clinical Neurophysiology 110 (1999) 660–665

Short communication

A ring-shaped distribution of dipoles as a source model of induced gamma-band activity

C. Tallon-Baudry, O. Bertrand, J. Pernier*

Mental Processes and Brain Activation, Institut National de la Santé et de la Recherche Médicale U280, F-69424 Lyon Cedex 03, France

Accepted 26 August 1998

Abstract

As opposed to slow waves, spontaneous and stimulus-induced oscillations in the gamma-band show no polarity reversal in cortical depth, which cannot be explained by the classical equivalent current dipole model usually proposed as a model of pyramidal cell synaptic activity. Here we propose a ring-shaped distribution of dipoles as a source model for these fast oscillations. This distribution generates a field potential that does not reverse through cortical depth. Such a geometry could correspond to horizontally oriented dendritic fields. Moreover, this distribution generates a potential field, but no, or weak, magnetic field on the scalp surface, which corresponds to the observation that visually-induced gamma-band oscillations are detectable in EEG data, but not in simultaneously recorded MEG data. © 1998 Elsevier Science Ireland Ltd. All rights reserved.

Keywords: Oscillations; Gamma rhythm; 40 Hz; Potential field; Current source density; Interneurons

1. Introduction

Epochs of oscillatory synchronization in the gamma-band (30–70 Hz) have been described in a variety of species and experimental conditions, and have been suggested to play a functional role in binding (for review see König and Engel, 1995; Singer and Gray, 1995). Nevertheless, several types of fast oscillatory synchronous activity can be differentiated (Galambos, 1992; Steriade et al., 1996): spontaneous, stimulus-induced (appearing with a jitter in latency from one trial to the next), and stimulus-locked or evoked activity (appearing at a fixed latency on successive trials). The issue of the neuronal circuitry generating these synchronized oscillations remains open. In this paper, we shall focus on the cortical generators of spontaneous and stimulus-induced fast oscillations.

Steriade and Amzica (1996) and Steriade et al. (1996) reported the existence of spontaneous or stimulus-induced fast oscillations in motor, somatosensory and association areas of anaesthetized cats. In most cases these fast oscillations do not show any polarity reversal in the depth of the cortex. They are probably not due to volume conduction of distant active structures: their amplitudes decrease significantly in the underlying white matter, and their negative fields are associated with neuronal firing in both upper and deeper layers. The cortical profile of gamma-band oscillations induced by a moving bar in cat's area 17 does not show any polarity reversal either (Eckhorn et al., 1998; Gray, unpublished data).

On the contrary, spontaneous or stimulus-induced slow waves are often reversed across the cortex (Steriade and Amzica, 1996; Steriade et al., 1996). The same holds true for most early components of the averaged evoked potential (Mitzdorf, 1991). The phase-reversals are mainly due to the activity of vertically oriented dendritic fields, like those of pyramidal cells (Nunez, 1981). The transmembrane primary currents that generate this type of phase-reversed field can be approximated by equivalent current dipoles perpendicular to the cortical surface.

Here we propose a simple ring-shaped distribution of equivalent dipoles able to produce a local field that shows no polarity reversal across the conducting medium in a limited area. This model is a distribution of current dipoles oriented tangentially with respect to the surface of the conducting medium, and radially distributed on a circumference (Fig. 1A). This model may account for the absence of polarity reversal observed in cats. Furthermore, it may also account for the discrepancy we observed in humans between electro-encephalographic (EEG) and magneto-encephalographic (MEG) data (Tallon-Baudry et al., 1997). Indeed, while visually induced gamma-band oscilla-

* Corresponding author. Tel.: + 33-472-68-19-03; fax: + 33-472-68-19-02.

E-mail address: pernier@lyon151.inserm.fr (J. Pernier)

PII: S1388-2457(98)00008-X

CLINPH 98616

tions are detectable in EEG data, they are not in simultaneously recorded MEG data, as opposed to visually evoked oscillatory responses which can be observed also in MEG recordings (Lopez and Sannita, 1997; Tallon-Baudry et al., 1997). Furthermore, in a motor task, the amplitude variations of induced 40 Hz activity around movement onset was found to be larger in EEG than in MEG recordings (Salenius et al., 1996 ; Pfurtscheller et al., 1997). The current dipole distribution proposed here generates an electrical field, but no, or weak, magnetic field, outside the conducting medium.

2. Field pattern of the current distribution

The potential field generated by a distribution of current equivalent dipoles is usually determined in a spherical volume conductor. Nevertheless, no simple analytical expression to compute the electrical potential exists in the case of a distribution of tangential dipoles radially distributed on a circumference. As a first approximation, we can neglect the curvature of the brain and surrounding tissues and compute the electrical field generated in a semi-infinite plane conducting medium, this approximation being valid in the vicinity of the current generators.

Let us consider a uniform distribution of radial current dipoles with a moment per unit length dl equal to ν on a circumference of radius a (Fig. 1A). We consider the dipoles oriented outward. The results are equally valid for a ring of dipoles oriented inward – it indeed only requires changing the sign of the potential values. Let us suppose that this distribution is located in an infinite medium of conductivity σ_1. The electric potential value at a point $P(z,R)$ is given by (Durand, 1996):

$$V(z,R) = \frac{V(0,0)}{\pi}\cdot\frac{a}{r}\cdot\left\{J_1(k) + \frac{a^2 - R^2 - z^2}{(a-R)^2 + z^2}\cdot J_2(k)\right\}$$

with:

$$V(0,0) = -\frac{\nu}{2a\sigma_1}$$

$$r = \sqrt{z^2 + (a+R)^2}$$

$$k = \frac{2\sqrt{aR}}{r}$$

$J_1(k)$ and $J_2(k)$ are the elliptic integrals of the first and the second kind:

$$J_1(k) = \int_0^{\frac{\pi}{2}} \frac{d\psi}{\sqrt{1 - k^2\sin^2\psi}}$$

$$J_2(k) = \int_0^{\frac{\pi}{2}} \sqrt{1 - k^2\sin^2\psi}\cdot d\psi$$

These integrals can be approximated by analytical functions with errors, respectively, inferior to 2×10^{-7} and 4×10^{-4} in the range $0 \leq k < 1$ (Hastings, 1955).Now let us assume that the current dipole distribution is placed in a semi-infinite medium of conductivity σ_1, limited by a plane boundary, the above conductivity being $\sigma_2 = 0$. Let h be the distance from the distribution center to the plane. The potential in the conducting medium can be calculated by the method of images. This potential is given by the superposition of the potentials created by two distributions:

$$V = V_1 - A\cdot V_2$$

V_1 is the potential created by the distribution placed in the semi-infinite medium of conductivity σ_1. V_2 the potential created by the same distribution, but placed at a distance h above the boundary plane.

$$A = \frac{\sigma_2 - \sigma_1}{\sigma_2 + \sigma_1} = -1$$

A cross-section of this potential field passing through the center of the distribution is represented in Fig. 1B. The potential does not reverse throughout the depth of the conducting medium, inside a cylinder of radius a and whose axis is passing through the center of the current dipole distribution. A maximum of potential can be observed at the depth of the current distribution. As the*s*

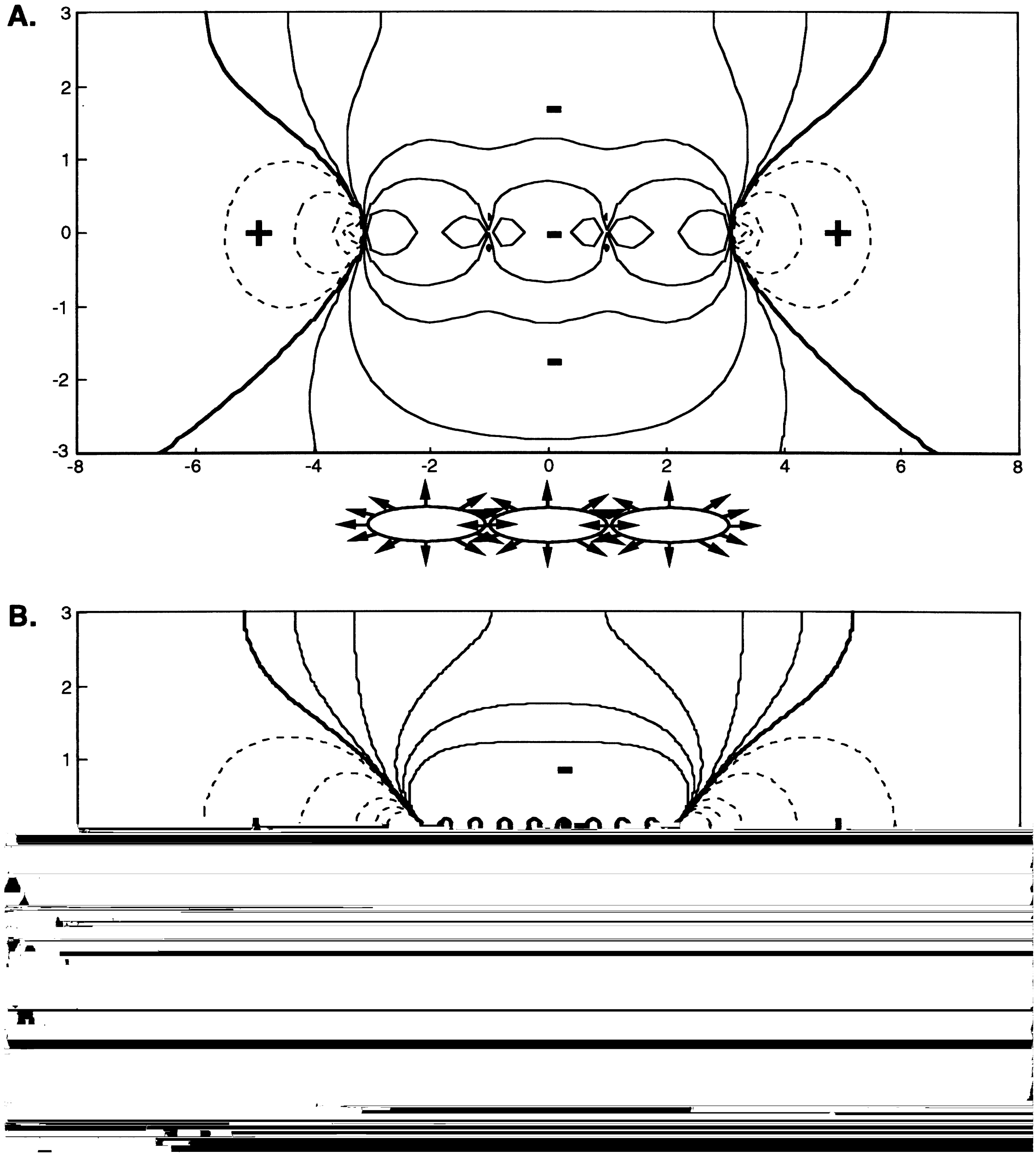

Fig. 2. (A) Alignment of 3 ring-shaped source distributions along the horizontal axis. The reversal-free area is increased as compared with Fig. 1B. (B) Combination of 9 parallel quadrupoles. Although this configuration increases the area of negative polarity along the horizontal axis, very focal polarity reversal still exists near the sources.

ratio h/a decreases, the global characteristics of the field potential distribution in depth are not modified. Outside this cylinder, the potential reverses twice in depth (for instance, as R = 2 in Fig. 1B).

In order to compare the depth profiles of 'current-source-density' (CSD) observed by Steriade and Amzica (1996), the second derivative of the potential has been computed along a vertical axis (dashed line in Fig. 1B). The depth profile of this second derivative shows alternatively positive and negative values across cortical layers (Fig. 1C).

It should be noted that the potential at point P due to a ring-shaped distribution can also be expressed, in spherical coordinates, as the following multipole expansion:

$$V(\rho,\theta) = V(0,0)\left[\left(\frac{a}{\rho}\right)^3 P_2(\cos\theta) - \frac{3}{2}\left(\frac{a}{\rho}\right)^5 P_4(\cos\theta) + \ldots\right]$$

where ρ is the distance between P and the center O of the ring, θ the angle between OP and the z axis, and $P_n()$ the Legendre Polynomial of degree n. This means that, at distance from the ring, the first term of the series is dominating, and the field distribution of ring-shape sources becomes equivalent to that of a quadrupole, i.e. two very

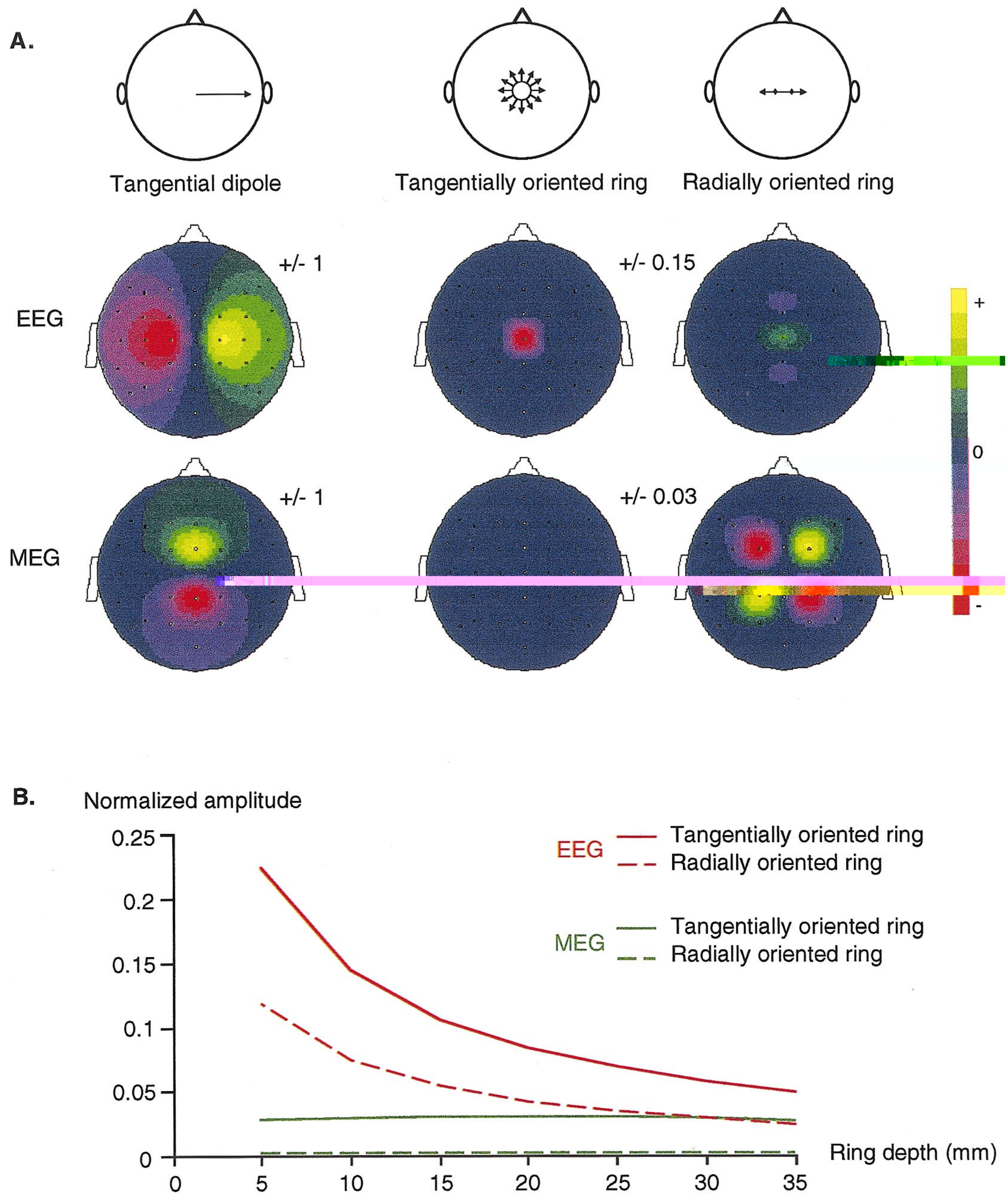

Fig. 3. (A) Electrical and magnetic topographies generated by a tangential dipole (left column), 16 dipoles distributed along a ring oriented tangentially with respect of the scalp surface (middle), or oriented radially with respect to the scalp surface (right column). Each of the 16 dipoles has a moment of 1/16th the tangential dipole moment. Scales are normalized by the maximum amplitude value of the distribution generated by the single tangential dipole. The potential distribution generated by the ring is reduced to 15% and the magnetic field to 3%. In this example, ring radius a = 3 mm, and depth below inner skull = 10 mm. (B) Variation with ring depth of the normalized amplitude of the potential (red) and magnetic (green) field, generated by a tangentially oriented (solid line) or radially oriented (dashed line) ring.

close dipoles of same magnitude located at the center of the ring, perpendicular to it and of opposite direction.

To explain the measured field potential depth profiles without polarity reversal, reported by Steriade and Amzica (1996) and Steriade et al. (1996) (Fig. 3), one may consider a combination of ring-shaped sources along the horizontal axis of the cortex (Fig. 2A), as well as a combination of parallel quadrupoles (Fig. 2B). Both source configurations will enlarge the reversal-free region in a given cortical area. As opposed to ring-shaped sources, the combination of quadrupoles still create a focal double inversion pattern.

3. Magnetic eld generated b a ring-shaped distribution

To determine the magnetic field generated by such a current distribution, Ampere's law can be used to determine the magnetic field $\vec{B}$ from currents. The current distribution $\vec{j}$

HJ. Coherent oscillations: a mechanism of feature linking in the visual cortex? Biol Cybern 1998;60:121–130.
Galambos R. A comparison of certain gamma-band (40 Hz) brain rhythms in cat and man. In: Basar E, Bullock TH, editors. Induced rhythms in the brain, Boston: Birhäuser, 1992. pp. 201.
Gray CM, McCormick DA. Chattering cells: superficial pyramidal neurons contributing to the generation of synchronous oscillations in the visual cortex. Science 1996;274:109–113.
Hastings C. Approximations for digital computers. Princeton: Princeton University Press, 1955.
Jagadeesh B, Gray CM, Ferster D. Visually evoked oscillations of membrane potential in cells of cat visual cortex. Science 1992;257:552–554.
König P, Engel AK. Correlated firing in sensory-motors systems. Curr Opin Neurobiol 1995;5:511–519.
Llinãs R. The intrinsic electrophysiological properties of mammalian neurons: insights into central nervous system function. Science 1988;242:1654–1664.
Lopez L, Sannita WG. Magnetically recorded oscillatory responses to luminance stimulation in man. Electroenceph clin Neurophysiol 1997;104:91–95.
Mitzdorf U. Physiological sources of evoked potentials. In: Brunia CHM, Mulder G, Verbaten MN, editors. Event-related brain research (EEG Suppl. 42), Amsterdam: Elsevier, 1991. pp. 47.
Nunez PL. Electric fields of the brain. New York: Oxford University Press, 1981.
Pfurtscheller G, Stancak A, Edlinger G. On the existence of different types of central beta rhythms below 30 Hz. Electroenceph clin Neurophysiol 1997;102:316–325.
Salenius S, Salmelin R, Neuper C, Pfurtscheller G, Hari R. Human cortical 40 Hz rhythm is closely related to EMG rhythmicity. Neurosci Lett 1996;21:75–78.
Sarvas J. Basic mathematical and electromagnetic concepts of the biomagnetic inverse problem. Phys Med Biol 1987;32:11–22.
Singer W, Gray CM. Visual feature integration and the temporal correlation hypothesis. Annu Rev Neurosci 1995;18:555–586.
Steriade M, Amzica F. Intracortical and corticothalamic coherency of fast spontaneous oscillations. Proc Natl Acad Sci USA 1996;13:2533–2538.
Steriade M, Amzica F, Contreras D. Synchronization of fast (30-40 Hz) spontaneous cortical rhythms during brain activation. J Neurosci 1996;16:392–417.
Tallon-Baudry C, Bertrand O, Wienbruch C, Ross B, Pantev C. Combined EEG and MEG recordings of visual 40 Hz responses to illusory triangles in human. NeuroReport 1997;8:1103–1107.
Wang XJ, Buzsaki G. Gamma oscillation by synaptic inhibition in a hippocampal interneuronal network model. J Neurosci 1996;15:6402–6413.
Whittington MA, Traub RD, Jefferys JGR. Synchronized oscillations in interneuron networks driven by metabotropic glutamate receptor activation. Nature 1995;373:612–615.